Cation−Ether Complexes in the Gas Phase: Bond Dissociation Energies of Na^+(dimethyl ether)$_x$, $x = 1-4$; Na^+(1,2-dimethoxyethane)$_x$, $x = 1$ and 2; and Na^+(12-crown-4)

Michelle B. More,[†] Douglas Ray,*[,‡] and P. B. Armentrout*[,†]

Department of Chemistry, University of Utah, Salt Lake City, Utah 84112, and Environmental Molecular Sciences Laboratory, Pacific Northwest National Laboratory, Richland, Washington 99352

Received: September 17, 1996; In Final Form: October 29, 1996[⊗]

Bond dissociation energies of $Na^+[O(CH_3)_2]_x$, $x = 1-4$; $Na^+[(CH_2OCH_3)_2]_x$, $x = 1$ and 2; and $Na^+[c\text{-}(C_2H_4O)_4]$ are reported. The bond dissociation energies are determined experimentally by analysis of the thresholds for collision-induced dissociation of the cation−ether complexes by xenon measured using guided ion beam mass spectrometry. In all cases, the primary and lowest energy dissociation channel observed experimentally is endothermic loss of one ligand molecule. The cross section thresholds are interpreted to yield 0 and 298 K bond dissociation energies after accounting for the effects of multiple ion−molecule collisions, internal energy of the complexes, and unimolecular decay rates. Trends in the bond dissociation energies determined by experiment and recent theoretical *ab initio* calculations are in good agreement. Our best experimental values, which have an average uncertainty of ±7 kJ/mol, are lower than the theoretical values by 7 ± 5 kJ/mol per metal−oxygen interaction. These values are compared with bond dissociation energies for the comparable lithium cation−ether complexes. This comparison reveals the thermodynamic consequences of ligand−ligand repulsion.

Introduction

Scientists have long been fascinated with understanding the interaction between ions and neutral molecules as it relates to molecular recognition in condensed phases.[1,2] One difficulty in this endeavor is separating the intrinsic interaction between the ion and the neutral molecule from those mediated by solvent molecules. One obvious way to achieve this separation is to work in the gas phase, a solvent-free environment. There, the intrinsic ion−neutral interactions can be determined and later combined with data on ion solvation[3,4] to better characterize the condensed phase phenomena.

There have recently been a number of studies concerning ion−crown ether complexes, one of the simplest molecular recognition systems, in the gas phase. Brodbelt and co-workers[5] have studied alkali ion selectivities of crown ethers via the kinetic method[6] and made qualitative conclusions about the alkali ion−crown bonding. Dearden and co-workers[7−9] have studied the interactions of alkali ions with crown ethers and acyclic glymes using ion cyclotron resonance (ICR) mass spectrometry and tandem quadrupole mass spectrometry. Using the former technique, they have studied the rates of ion−ligand complexation reactions. Using the latter method, ion−ligand selectivities were determined by the kinetic method and found to differ in some cases from those determined with the ICR. These studies have begun to provide insight into the alkali ion−crown ether complexes, but they also point to a lack of quantitative information regarding these species and their bonding.

It is the purpose of this study to provide quantitative values for the binding energies of Na^+ to 12-crown-4 (12c4), *c*-$(C_2H_4O)_4$. To assess the accuracy of the collision-induced dissociation (CID) method used here and to examine effects associated with preorganized multidentate ligands, we also determine the thermochemistry for dimethyl ether (DME) complexes, $Na^+[O(CH_3)_2]_x$, $x = 1-4$, and 1,2-dimethoxyethane (DXE) complexes, $Na^+[(CH_2OCH_3)_2]_x$, $x = 1$ and 2. These results are then compared with recent theoretical results[10,11] and with similar data previously obtained for the comparable complexes with Li^+.[12,13]

Experimental Section

Complete descriptions of the apparatus and the experimental procedures are given elsewhere.[14,15] The production of $Na^+(L)_x$ (L = DME, DXE, and 12c4) complexes is described below. Briefly, ions are extracted from the source, accelerated, and focused into a magnetic sector momentum analyzer for mass analysis. Mass-selected ions are retarded to a desired kinetic energy and focused into an octopole ion guide that radially traps the ions. The octopole passes through a static gas cell containing xenon, used as the collision gas for reasons described elsewhere.[16,17] After exiting the gas cell, product and unreacted reactant ions drift to the end of the octopole, where they are focused into a quadrupole mass filter for mass analysis and subsequently detected by a secondary electron scintillation ion counter using standard pulse-counting techniques. Raw ion intensities are converted to absolute cross sections as described previously.[14] Absolute uncertainties in cross section magnitudes are estimated to be ±20%, and relative uncertainties are ±5%.

Ion kinetic energies in the laboratory frame are related to center-of-mass (CM) frame energies by $E(\mathrm{CM}) = E(\mathrm{lab})m/(M + m)$, where M and m are the ion and neutral reactant masses, respectively. All energies cited below are in the CM frame unless otherwise noted. Sharp features in the observed cross sections are broadened by the thermal motion of the neutral gas[18] and the distribution of ion energies. The zero of the absolute energy scale and the full width at half maximum (fwhm) of the ion energy distribution are measured by a retarding potential technique described elsewhere.[14] The fwhm of the ion beam energy distribution was typically between 0.3 and 0.6 eV (lab) for these experiments. The uncertainty in the absolute energy scale is ±0.05 eV (lab).

The complexes are formed in a 1 m long flow tube[15] operating at a pressure of 0.4−0.7 Torr with a helium flow rate of 4000−

[†] University of Utah.
[‡] Pacific Northwest National Laboratory.
[⊗] Abstract published in *Advance ACS Abstracts,* January 1, 1997.

S1089-5639(96)02851-4 CCC: $14.00

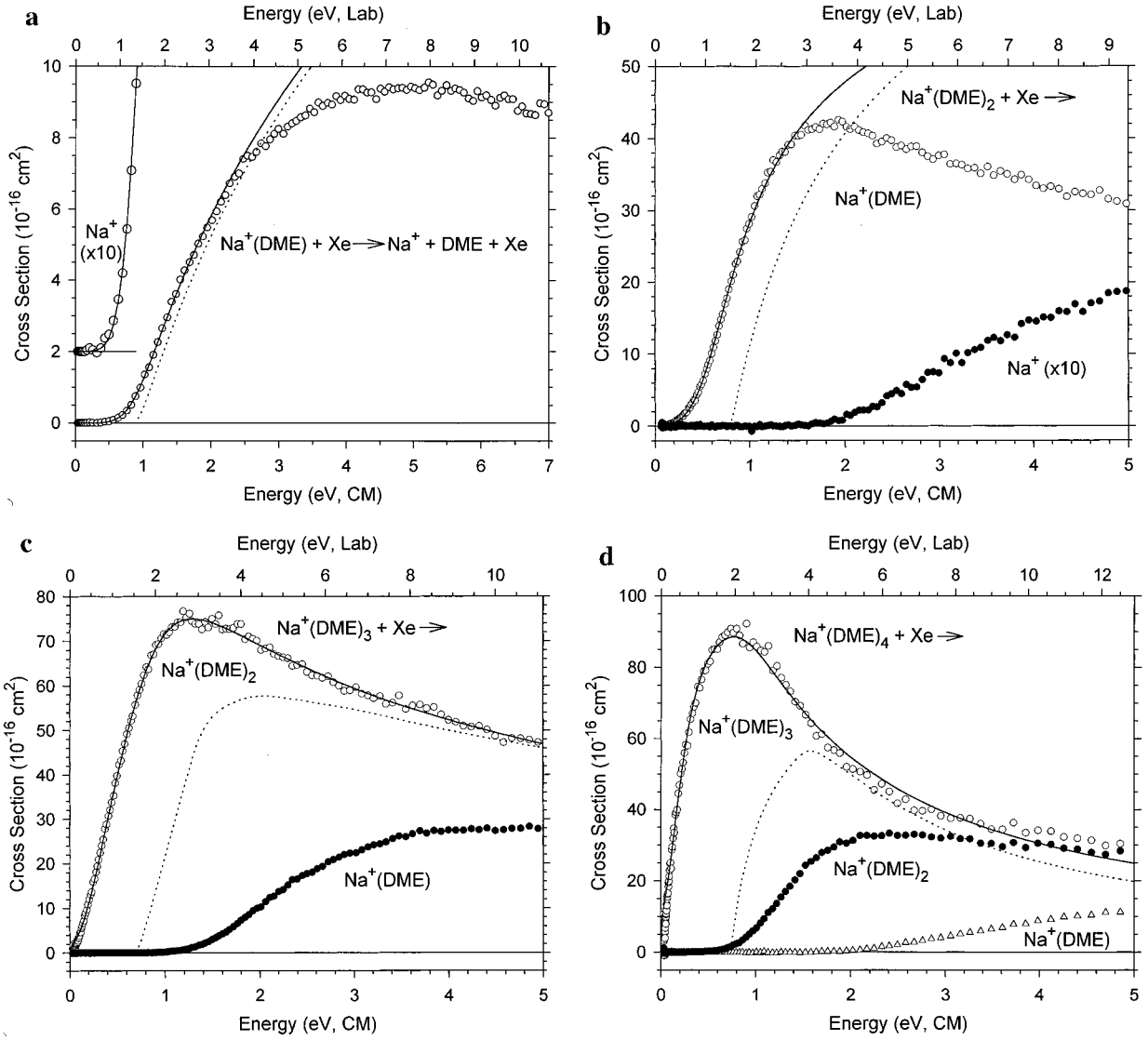

Figure 1. Cross sections for reactions of $Na^+(DME)_x$, $x = 1-4$, with xenon (parts a−d, respectively) as a function of kinetic energy in the center-of-mass frame (lower *x* axis) and the laboratory frame (upper *x* axis). Open circles, filled circles, and open triangles show cross sections for the primary, secondary, and tertiary products, respectively. The best fits to the data using the model of eq 3 incorporating RRKM modeling for the reactants with an internal temperature of 0 K are shown as dotted lines. Solid lines show these models convoluted over the neutral and ionic kinetic and internal energy distributions.

9000 standard cm^3/min. Sodium ions are generated in a continuous dc discharge by argon ion sputtering of a cathode consisting of a carbon steel "boat" containing sodium metal. Complexes are formed by three-body associative reactions with the desired ligand introduced to the flow 5 cm downstream from the dc discharge. Typical operating conditions of the discharge are 3 kV and 30 mA in a flow of 5−15% argon in helium. The flow conditions used in this source provide approximately 10^5 collisions between the ions and the buffer gas, which should thermalize the complexes both rotationally and vibrationally to 300 K, the temperature of the flow tube. Previous work by Armentrout and co-workers[19−23] has shown that this assumption is reasonable and no evidence for nonthermal ions was observed in this work.

Experimental Results

$Na^+(DME)_x$, $x = 1-4$. Experimental cross sections for the collision-induced dissociation (CID) of the $Na^+(DME)_x$, $x = 1-4$, ion−molecule complexes are shown in Figures 1a−d. The sequential loss of intact DME molecules and ligand exchange with xenon to form $Na^+(Xe)$ are the only processes observed in these systems over the collision energy range studied, typically 0−10 eV. The cross sections for ligand exchange are small, and thus data for these channels were not collected. The primary (both the lowest energy and dominant) process for all complexes is the loss of a single DME ligand in reaction 1.

$$Na^+(DME)_x + Xe \rightarrow Na^+(DME)_{x-1} + DME + Xe \quad (1)$$

As *x* increases, the primary cross section begins to decline more rapidly at higher energies because pathways for the primary product to decompose further become more efficient. All complexes dissociate completely to the bare metal cation at high energies. Na^+ product channels are not shown in Figure 1c,d because they have relatively small cross sections. The apparent thresholds of these cross sections are at about 2.5 and 5 eV, respectively, with maximum magnitudes of about 3 and <0.6 Å^2, respectively, at energies > 6 eV. The shapes of the cross sections and the reaction pathways for the $Na^+(DME)_x$, $x = 1-4$, complexes are very similar to those of the previously studied $Li^+(DME)_x$ analogues.[12]

$Na^+(DXE)_x$, $x = 1$ and 2. Experimental cross sections for CID of the $Na^+(DXE)_x$, $x = 1$ and 2, ion−molecule complexes are shown in Figure 2a,b. The cross sections for ligand

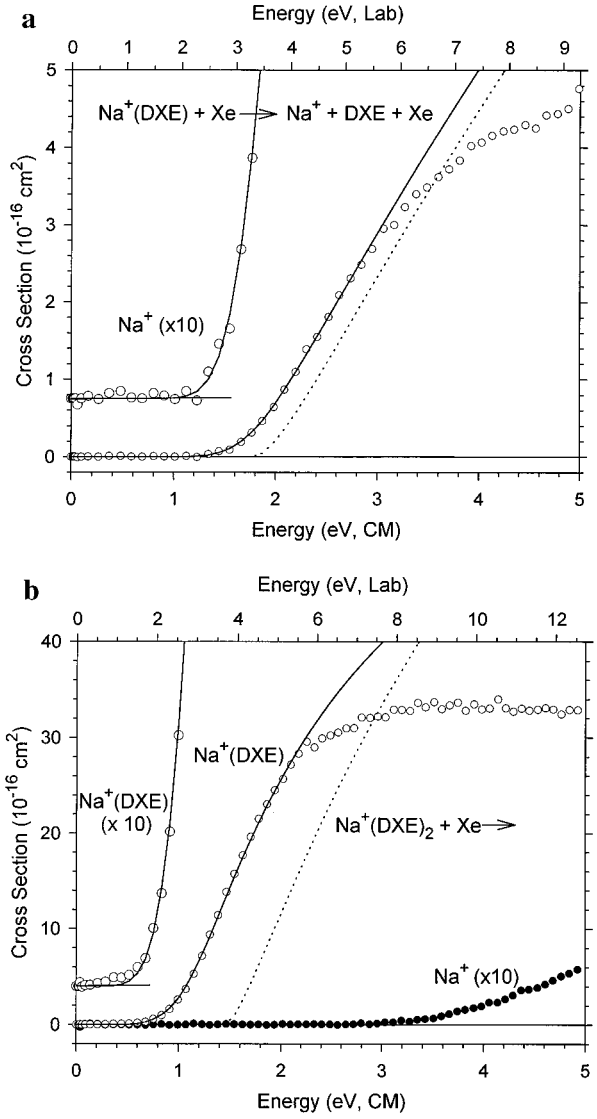

Figure 2. Cross sections for reactions of $Na^+(DXE)_x$, $x = 1$ and 2, with xenon (parts a and b, respectively) as a function of kinetic energy in the center-of-mass frame (lower x axis) and the laboratory frame (upper x axis). Open and filled circles show cross sections for the primary and secondary products, respectively. The best fits to the data using the model of eq 3 incorporating RRKM modeling for the reactants with an internal temperature of 0 K are shown as dotted lines. Solid lines show these models convoluted over the neutral and ionic kinetic and internal energy distributions.

exchange are small, and thus data for these channels were not collected. The lowest energy and dominant process for all complexes is the loss of a single DXE ligand in reaction 2.

$$Na^+(DXE)_x + Xe \rightarrow Na^+(DXE)_{x-1} + DXE + Xe \quad (2)$$

At energies greater than 7 eV, the $Na^+(DXE)$ complex also yields ligand fragmentation products, $Na^+(OCH_2)$ and $Na^+[(CH_3)_2O]$, with maximum cross sections of 0.08 and 0.05 Å^2, respectively. The $Na^+(DXE)_2$ complex loses both DXE ligands at elevated energies, but this process is inefficient. Again, the CID of $Na^+(DXE)_x$, $x = 1$ and 2, complexes with xenon follows similar reaction pathways with comparable cross section shapes when compared with the CID of $Li^+(DXE)_x$, $x = 1$ and 2.[13]

Na^+(12c4). Results for the interaction of Na^+(12c4) with xenon are shown in Figure 3. No products other than Na^+ and ligand exchange to form Na^+(Xe) are observed. This behavior is in contrast to the CID results of Li^+(12c4).[13] In that work, production of Li^+ was the dominant product, but cleavage of

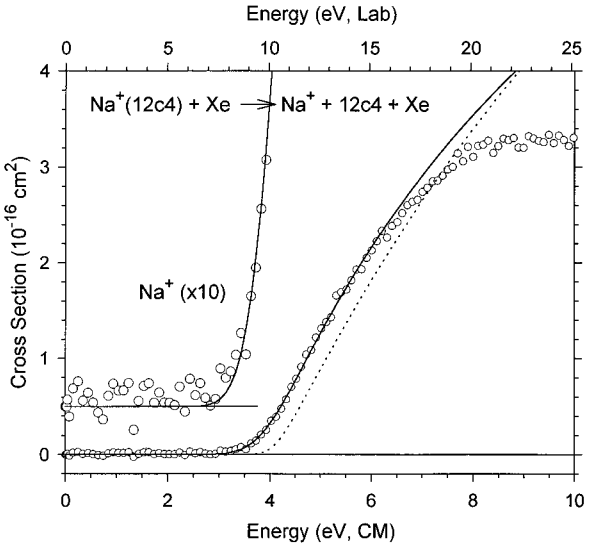

Figure 3. Cross sections for the reaction of Na^+(12c4) with xenon as a function of kinetic energy in the center-of-mass frame (lower x axis) and the laboratory frame (upper x axis). Open circles show cross sections for the primary product ion. The best fit to the data using the model of eq 3 incorporating RRKM modeling for the reactants with an internal temperature of 0 K is shown as a dotted line. The solid line shows this model convoluted over the neutral and ionic kinetic and internal energy distributions.

the ligand was also observed. These latter products included $Li^+(C_3H_6O_2)$, the product having the lowest energy threshold, as well as $Li^+(CH_2O)$, $Li^+(C_2H_4O)$, and $Li^+(C_2H_4O_2)$, which appear at higher energies. Similar products in the Na^+ system were looked for but not observed, indicating that they have cross sections less than 10^{-18} cm^2 over the energy range studied.

Thermochemical Analysis

Cross sections are modeled in the threshold region with eq 3,

$$\sigma = \sigma_0 \sum g_i (E + E_i + E_{rot} - E_0)^n / E \quad (3)$$

where σ_0 is an energy independent scaling factor, E is the relative translational energy of the reactants, E_0 is the threshold energy for reaction of the ground rotational, vibrational, and electronic state, E_{rot} is the rotational energy of the reactants ($3k_BT/2 = 0.039$ eV for all species studied here), and n is an adjustable parameter. The summation is over i, which denotes the vibrational states of the complex, g_i is the population of those states ($\Sigma g_i = 1$), and E_i is the excitation energy of each vibrational state. Because the complexes studied here have many low-frequency vibrational modes, the populations of excited vibrational levels are not negligible even at 298 K. The Beyer−Swinehart algorithm[24] is used to calculate the population of the vibrational levels using the frequencies listed in Table 1. Vibrational frequencies for all sodium complexes, free 1,2-dimethoxyethane, and free 12c4 are taken from theoretical calculations of Feller and co-workers[10,11] and scaled by 85, 90, and 100%. The corresponding change in the *average* vibrational energy is taken to be an estimate of one standard deviation of the uncertainty in vibrational energy. Frequencies for free DME have been taken from Shimanouchi.[25]

The form of eq 3 is expected to be appropriate for translationally driven reactions[26] and has been found to reproduce cross sections well in a number of previous studies of both atom−diatom and polyatomic reactions[27,28] including CID processes.[3,17,20] Because the rotational, vibrational, and translational

TABLE 1: Vibrational Frequencies and Average Vibrational Energies at 298 K[a]

species	E_{vib},[b] eV	Frequencies(degeneracies), cm^{-1}
DME	0.04	203, 242, 418, 928, 1102, 1150, 1179, 1227, 1244, 1452(2), 1464(4), 2817(2), 2925, 2952, 2996(2)
Na^+(DME)	0.094(0.00)	**100**, **106**, 165, 229, 248, 417, 892, **1067**, 1145, 1167, 1180, 1264, 1451, 1464, 1478, 1482, 1489, 1493, 2905, 2911, 2985(2), 2987, 2988
Na^+(DME)$_2$	0.27(0.01)	**9**, **13(2)**, **93(2)**, 110(2), 128, 170, 246(2), **272**, 412, 417, 895, 900, 1073(2), 1145(2), 1171(2), 1180(2), 1265(2), 1452(2), 1465(2), 1479(2), 1483(2), 1488(2), 1493(2), 2902(2), 2907, 2908, 2977(2), 2978(2), 2984(2), 2986(2)
Na^+(DME)$_3$	0.45(0.02)	**13(2)**, **20(2)**, **23**, 24, 88(2), 96(2), 117, 121, 175(2), **230**(2), 243, 245(2), 410, 411(2), 901(2), 910, 1080, 1081(2), 1148(3), 1176(3), 1181(3), 1265(3), 1451, 1452(2), 1467(2), 1469, 1480, 1481(2), 1484(3), 1487(3), 1494(2), 1495, 2896(3), 2903(3), 2966(3), 2967(3), 2984(3), 2986(3)
Na^+(DME)$_4$	0.62(0.02)	**16(2)**, **18**, **21**, **29**, 32, 35(2), 36, 79, 82(2), 86, 92, 96(2), 99, 113, 178, 180(3), **201**(2), 214, 242, 243, 245, 409(4), 907(3), 919, 924, 1086(3), 1148(4), 1180, 1182(7), 1265(4), 1450(3), 1452, 1469(3), 1472, 1482(4), 1484(4), 1485, 1486(3), 1495(2), 1496, 1497, 2891(3), 2892, 2899(3), 2900, 2957(8), 2985(4), 2989(4)
DXE	0.14(0.01)	68, 110, 118, 144, 209, 229, 319, 383, 487, 814, 955, 1006, 1055, 1140, 1155, 1164, 1167, 1180, 1224, 1232, 1238, 1286, 1357, 1444, 1467, 1478, 1481(2), 1490, 1491, 1509, 1516, 2862, 2863, 2875, 2876, 2893, 2911, 2918(2), 2984, 2985
Na^+(DXE)	0.19(0.01)	48, 108, 116, 147, 190(2), **212**, **217**, 284, 344, 362, **543**, 828, 855, 1004, 1029, 1087, 1111, 1125, 1162, 1167, 1209, 1226, 1260, 1298, 1396, 1436, 1469, 1473, 1474, 1475, 1486, 1487, 1497, 1501, 2901, 2902, 2907, 2908, 2946, 2957, 2975(2), 2999(2)
Na^+(DXE)$_2$	0.46(0.02)	**10**, **21(2)**, 47(2), **84**, 104(2), 108, 117, 144, 145, 172(2), 195, **196**, **212**(2), 247, 281(2), 334(2), 349, 360, 547(2), 835(2), 857, 861, 1009, 1013, 1033(2), 1103(2), 1112(2), 1135(2), 1164(2), 1168(2), 1212, 1213, 1227(2), 1259(2), 1296(2), 1396, 1436(2), 1469(2), 1473(2), 1475(3), 1475, 1476, 1486(2), 1487(2), 1499(2), 1502(2), 2891(2), 2894(2), 2899(2), 2903(2), 2933(2), 2944(2), 2962(4), 2993(4)
12c4	0.27(0.02)	60, 82, 126(2), 146(2), 232, 241(2), 297, 346, 353(2), 363, 460, 517(2), 558, 778, 814(2), 858, 898, 912(2), 933, 1017, 1039(2), 1045, 1094, 1120(2), 1140, 1173, 1176(2), 1184, 1256, 1264, 1270, 1286, 1308(2), 1326, 1372, 1391(2), 1409, 1425, 1435(2), 1438, 1482(2), 1483, 1484, 1494(3), 1500, 2857(3), 2858, 2892, 2894(2), 2897, 2935, 2936(2), 2937, 2959, 2960(2), 2963
Na^+(12c4)	0.29(0.02)	64, 113, **149**, 175(2), **183**, **195**(2), 203, 235, 275(2), 295, 340, 354(2), 394, 479, 536(2), 581, 780, 801(2), 850, 891, 904, 911(2), 1022, 1032(2), 1050, 1063, 1108(2), 1130, 1148, 1155(2), 1167, 1249, 1257(2), 1269, 1277, 1301(2), 1313, 1366, 1386(2), 1402, 1427, 1428, 1429(2), 1483, 1484(2), 1485, 1494, 1501(2), 1512, 2892, 2900(2), 2905, 2921, 2923(2), 2927, 2937, 2939(2), 2945, 2979(3), 2980

[a] RHF frequencies are taken from refs 10 and 11 scaled by 0.9. Transitional mode frequencies are in boldface, with the reaction coordinate being the largest of these values. [b] Uncertainties, listed in parentheses, are determined as described in the text.

energy distributions are explicitly included in our modeling, the threshold energies determined using eq 3 correspond to 0 K.

In our analysis of $Na^+(DME)_x$, $x = 3$ and 4, we also use a modified form of eq 3 that accounts for a decline in the product ion cross section at higher kinetic energies. This model has been described in detail previously[29] and depends on E_D, the energy at which a dissociation channel opens, and p, a parameter similar to n in eq 3.

Other considerations in the analysis of CID thresholds are the presence of nonthermal ions, pressure effects, and the lifetime of the complex.[20] These considerations are treated as follows. First, excess internal excitation is unlikely because the ions that traverse the 1 m long flow tube are thermalized by the $\sim 10^5$ collisions they undergo with the buffer gases. Second, pressure effects due to multiple collisions with Xe are examined by performing the experiments at three different pressures. Pressure effects are eliminated, following a procedure developed previously,[30] by linearly extrapolating the cross sections to zero-pressure, rigorously single collision conditions. It is these cross sections that are further analyzed.

The lifetime effect is examined by incorporating RRKM theory into eq 3 as previously detailed.[21,31] The additional information necessary to implement this theory is the set of vibrational frequencies for the transition state (TS) associated with the dissociation. This choice is reasonably straightforward because the TS should be fairly loose and similar to the CID products. Thus, most of the frequencies are those of the products, $Na^+(L)_{x-1}$ + L, which are listed in Table 1. The six [three for Na^+(DME), Na^+(DXE), and Na^+(12c4)] transitional frequencies affected most severely as the ligand is removed are in boldface in Table 1 and chosen as follows. One Na^+-L stretching frequency is chosen as the reaction coordinate and removed. The five [two for Na^+(DME), Na^+(DXE), and Na^+-(12c4)] remaining frequencies (usually hindered rotations, bends, and torsions) of the Na^+(L) reactant are modified by dividing these frequencies by factors of 2 and 10 to give a range in the looseness of the TS, which is characterized by the entropy of activation, $\Delta S^\dagger$. The threshold energies obtained with these modified TS parameters are averaged to yield E_0(loose). We also determine an energy threshold for a "tight" TS, E_0(tight), by removing only the reaction coordinate frequency and leaving the other *reactant* frequencies unchanged. This procedure parallels that used to analyze CID data of Li^+ bound to DME, DXE, and 12c4.[12,13]

In recent work on $Li^+(H_2O)_x$, $x = 1-6$,[31] and Li^+ complexed with a variety of small alcohols,[32] Rodgers and Armentrout present a less arbitrary procedure (i.e., one without the need to guess transitional frequencies) for modeling the loose transition states appropriate for the dissociation of ion−molecule complexes. In this revised procedure,[33] which we refer to here as the phase space limit (PSL), most of the vibrational frequencies are assigned to those of the products and the transitional modes are described as free rotations and torsions. Because the molecular parameters of the TS are simply related to similar parameters for the products, they are generally known or easily estimated. The PSL model should provide a reasonable description of the dissociation of ion−molecule complexes because the TS for the reverse, barrierless association process is often accurately described as lying at the top of the centrifugal barrier.

Before comparison with experimental data, the model of eq 3 is convoluted with the kinetic energy distributions of the reactants.[14] The parameters σ_0, n, and E_0 are then optimized with a nonlinear least-squares analysis to give the best fit to the data. An estimate of the error in the threshold energy is obtained for variations in E_0 for different data sets, variations in the parameter n, variations associated with the uncertainties in the vibrational frequencies, and the error in the absolute energy scale. Uncertainties listed with the E_0(PSL), E_0(loose), and E_0(tight) values also include errors associated with variations

TABLE 2: Bond Dissociation Energies at 0 K and Entropies of Activation at 1000 K of $Na^+(DME)_x$, $x = 1-4$; $Na^+(DXE)_x$, $x = 1$ and 2; and $Na^+(12c4)$[a]

species	E_0,[b] eV	E_0 (PSL), eV	$\Delta S^\dagger$ (PSL), J/(mol K)	E_0 (loose), eV	$\Delta S^\dagger$ (loose), J/(mol K)	E_0 (tight), eV	$\Delta S^\dagger$ (tight), J/(mol K)
$Na^+(DME)$	0.96(0.05)	0.95(0.05)	30	*d*		*d*	
$Na^+(DME)_2$	0.88(0.07)	0.85(0.05)	18	0.84(0.07)	59(47)	0.80(0.06)	3
$Na^+(DME)_3$	0.82(0.11)	0.72(0.05)	46	0.72(0.06)	99(47)	0.60(0.04)	8
$Na^+(DME)_4$	c	0.63(0.04)	65	0.57(0.10)	113(47)	0.36(0.04)	10
$Na^+(DXE)$	2.01(0.25)	1.64(0.04)	44	1.58(0.07)	17(19)	1.51(0.10)	2
$Na^+(DXE)_2$	1.71(0.15)	1.20(0.08)	65	1.19(0.14)	74(47)	1.08(0.07)	14
$Na^+(12c4)$	4.01(0.24)	2.61(0.13)	64	2.37(0.21)	39(18)	1.97(0.16)	12

[a] Uncertainties (one standard deviation) are listed in parentheses. The average values for n used in eq 3 were 1.2 ± 0.3 and 1.3 ± 0.3 without and with RRKM lifetime analysis, respectively. [b] No RRKM lifetime analysis. [c] Data could not be modeled well without incorporating the RRKM lifetime effect into eq 3. [d] RRKM lifetime analysis had no effect.

in the time assumed for dissociation (10^{-4} s) by a factor of 2 and 1/2. Uncertainties for the E_0(loose) and $\Delta S^\dagger$(loose) values include variations in the transitional frequencies as mentioned above.

Threshold energies for CID processes are converted into 0 K bond dissociation energies (BDEs) by assuming that E_0 represents the energy difference between the reactants and the products at 0 K.[34] This requires that there are no activation barriers in excess of the endothermicity. This is generally true for ion−molecule reactions[27,35] and should be valid for the simple bond fission reactions studied here.[36]

To compare BDEs measured here with those determined in the literature, 0 K BDEs are converted to 298 K BDEs using the standard formulas for the temperature dependence of the enthalpy.[37] Following this method, BDEs for $Na^+(DME)_x$, $x = 1-4$, $Na^+(DXE)_x$, $x = 1$ and 2, and $Na^+(12c4)$ at 298 K are obtained by adding 0.9, −3.0, −2.8, −2.8, 0.1, −2.3, and 2.0 kJ/mol, respectively, to the 0 K BDEs.

Threshold Analysis. Results for the analysis of the cross sections shown in Figures 1−3 with eq 3 are provided in Table 2. In previous work, we have generally found that thresholds obtained assuming a *loose* TS provide the most accurate thermochemistry.[12,38] The *tight* TS values can be viewed as very conservative lower limits to the correct thermodynamics, while values obtained with no RRKM modeling provide very conservative upper limits. In our previous work on the $Li^+(DME)_x$ and $Li^+(DXE)$ complexes, our best experimental BDEs were concluded to be the E_0(loose) values. Here, we believe that the best experimental BDEs for the $Na^+(DME)_x$ and $Na^+(DXE)$ complexes are the E_0(PSL) values derived from our loosest TS model, for reasons noted above. In the case of $Li^+(12c4)$, the BDE is fairly high and fragmentation of the ligand was competitive with the dissociation of intact 12c4. Therefore, we concluded that the best experimental value for the $Li^+(12c4)$ BDE spanned the range of the E_0(loose) and E_0(tight) values. For the $Na^+(12c4)$ system, however, the BDE is lower and no ligand fragmentations are observed. Therefore, a loose TS model is more appropriate in this system, and for reasons noted above, we believe that the E_0(PSL) value is the most accurate BDE for $Na^+(12c4)$.

One useful measure of the looseness of the dissociation process is the change in entropy in going from reactants to the transition state during this process, $\Delta S^\dagger$. These values are listed in Table 2 for a temperature of 1000 K, often used as a standard.[39,40] The range of values obtained is similar to the results of a theoretical study on the dissociation dynamics of Na^+(18-crown-6) by Hase et al.[41] This investigation studied the complexation kinetics and dynamics of Na^+ with the D_{3d} and C_i conformations of 18-crown-6 using canonical variational transition state theory. Hase et al. explicitly examined how the transitional mode harmonic vibrational frequencies varied along the reaction path from the complex to the TS, correlating to a variation in the center-of-mass separation of 4−20 Å. They found that these frequencies decreased by factors of 4 (D_{3d} state) and 7 (C_i state) from the original complex frequencies. These factors are comparable with the range of 2−10 used in our *loose* TS mode modifications. Hase et al. also compute $\Delta S^\dagger$ at 300 K. For the D_{3d} state, $\Delta S^\dagger$ was calculated as 35 J/(mol K) and for the C_i state, $\Delta S^\dagger$ was 62 J/(mol K). At 300 K, the average calculated $\Delta S^\dagger$ for dissociation of $Na^+(12c4)$ is 84 J/(mol K) for our *PSL* TS, 49 ± 19 J/(mol K) for our *loose* TS, and 22 J/(mol K) for our *tight* TS. The similar ranges obtained in the two studies support the validity of our assumptions regarding the TS frequencies. They also point to a loose TS as being most reasonable for describing the dissociation of sodium ion−crown ether complexes.

Another way of assessing which model provides the most accurate thermochemistry is to examine trends in the relative kinetic shifts observed for the various complexes. The kinetic shift is the difference between the thresholds determined with and without including RRKM dissociation kinetics in the data analysis and can be obtained from the data in Table 2. In this study, no appreciable kinetic shift for $Na^+(DME)$ is observed, but all other complexes exhibit a small to significant correction for the lifetime effect. The kinetic shift increases with the number of ligands in the complex, consistent with large increases in the number of degrees of freedom available to the complex. The kinetic shifts also increase with the threshold energies, such that the greatest lifetime correction is for $Na^+(12c4)$. These trends have been noted before in other large systems including the CID of Li^+ with analogous ligands[13] and transition metal cluster ions.[42,43]

The trends in the lifetime corrections can be analyzed further by examining the equation used to incorporate an energy dependent unimolecular rate constant for dissociation into eq 3. The unimolecular rate constant is given by RRKM theory[44] as

$$k(E_T) = s\frac{Q^\dagger}{Q}\frac{N^\dagger(E_T - E_0)}{h\rho(E_T)} \qquad (4)$$

where $N^\dagger(E_T - E_0)$ is the sum of states of the TS at an energy $(E_T - E_0)$ above the dissociation energy, E_0, and $\rho(E_T)$ is the reactant density of states at the energy E_T. $Q^\dagger$ and Q are the rotational partition functions of the TS and the reactant, respectively. In the *PSL* model,[31] the $Q^\dagger/Q$ factor is deleted because the rotations of the energized molecule and the activated complex are handled explicitly in the calcuation of $N^\dagger(E_T - E_0)$ and $\rho(E_T)$. For dissociation of a species like $Na^+(L)_x$, the reactant path degeneracy s is equal to x. If we calculate the values for $N^\dagger(E_T - E_0)$ and $\rho(E_T)$ for the $Na^+(DME)_4$, $Na^+(DXE)_2$, and $Na^+(12c4)$ complexes at the same energy, we find that $Na^+(12c4)$ has a much smaller sum of states than the other two complexes because of the higher E_0 value. $Na^+(DME)_4$ and $Na^+(DXE)_2$ have larger values of $\rho(E_T)$ than $Na^+(12c4)$ at

all energies, but they also have compensatingly larger $N^{\dagger}(E_T - E_0)$ values. Overall, the ratio of $N^{\dagger}(E_T - E_0)$ to $\rho(E_T)$ for Na^+-(12c4) is several orders of magnitude smaller than the other two complexes, leading to a much slower unimolecular dissociation rate and hence a larger kinetic shift.

Discussion

Comparison of Experimental and Theoretical Bond Dissociation Energies. Table 2 compares the 0 K BDEs of the Na^+ complexes determined without RRKM modeling and with the three versions of the lifetime modeling. The threshold energies obtained without any lifetime analysis are the greatest, and the E_0(tight) values are the smallest. This is expected because these modeling procedures represent the shortest and longest lifetimes of the dissociating complexes, respectively. The E_0(loose) and E_0(PSL) values fall in between these end points. The E_0(PSL) BDEs are greater than the E_0(loose) BDEs and are generally consistent with the upper end of the uncertainties in these values. Qualitatively, the E_0(PSL) values are approximately the same as the E_0(loose) values where the transitional frequencies were scaled by a factor of 10. To assess which of these four E_0 values is most reliable, we can compare them with the theoretical values taken from the work of Feller et al.[10,11] In this theoretical work, equilibrium gas-phase geometries were optimized using a modified 6-31+G* basis set[45] at the second-order Møller−Plesset perturbation level of theory (MP2) for $Na^+(DME)_x$, $x = 1$ and 2, and at the restricted Hartree−Fock (RHF) level of theory for $Na^+(DME)_x$, $x = 3$ and 4, $Na^+(DXE)_x$, $x = 1$ and 2, and Na^+(12c4). Correlation corrections were evaluated with frozen-core MP2 theory applied to the optimized geometries. Basis set superposition errors in the calculated bond energies were corrected through the use of the counterpoise correction. As discussed in more detail below, a previous study of the analogous complexes of Li^+ with DME,[12] DXE, and 12c4[13] indicates that this level of theory provides fairly accurate thermodynamic information for such systems.

In all comparisons described in this paragraph, the experimental values from Table 2 are compared with theoretical results of Feller et al.[10,11] adjusted to 0 K. Neither the E_0 values without RRKM nor the E_0(tight) values agree well with theory, showing average deviations of 0.32 ± 0.59 eV above theory and 0.26 ± 0.16 eV below theory, respectively. Consistent with the observations made for the Li^+ complexes,[12,13] the E_0(loose) values agree much better with the theoretical results. These show an average deviation of 0.12 ± 0.08 eV below theory (0.08 ± 0.05 eV below if normalized by the number of oxygen atoms in the dissociating ligand). Our new modeling procedure yields E_0(PSL) values that agree slightly better with theory, with deviations of 0.07 ± 0.09 eV below theory (0.06 ± 0.06 eV below if normalized by the number of oxygen atoms). The largest difference between the loose and PSL values is observed for the 12c4 complex. E_0(PSL) is greater than E_0(loose) by 23 kJ/mol and is in much better agreement with the theory value. Because of this slightly better agreement and because there are fewer assumptions associated with choosing the molecular parameters for the PSL TS, we believe that the E_0(PSL) BDEs represent our best experimental values.

The comparison between the E_0(PSL) experimental values and the theoretical values of Feller et al.[10,11] is shown in Table 3 after adjusting both sets of values to 298 K enthalpies of dissociation for the DME, DXE, and 12c4 complexes with Na^+. The theoretical values generally exceed the experimental values except in the cases of $Na^+(DME)_4$ and Na^+(12c4). Discrepancies range from 2 to 15 kJ/mol for the monodentate ligands and from 5 to 15 kJ/mol for the multidentate ligands. When normalized by the number of oxygen atoms in the ligand, the average discrepancies are similar for both mono- and multidentate ligands, 7 ± 5 kJ/mol, within our average experimental uncertainty of ± 7 kJ/mol.

TABLE 3: Bond Dissociation Enthalpies at 298 K of $Na^+(DME)_x$, $x = 1-4$; $Na^+(DXE)_x$, $x = 1$ and 2; and Na^+(12c4) in kJ/mol[a]

species	ΔH_{298} (PSL)	ΔH_{298} (MP2)[b]
$Na^+(DME)$	93(5)	108
$Na^+(DME)_2$	79(5)	90
$Na^+(DME)_3$	67(5)	71
$Na^+(DME)_4$	58(4)	57
$Na^+(DXE)$	161(4)	176
$Na^+(DXE)_2$	114(8)	124
Na^+(12c4)	254(13)	249

[a] Uncertainties (one standard deviation) are listed in parentheses. [b] 6-31+G* values. The enthalpy corrections were determined using MP2 harmonic vibrational frequencies for $Na^+(DME)_x$, $x = 1$ and 2, and RHF harmonic vibrational frequencies scaled by 0.9 for $Na^+(DME)_x$, $x = 3$ and 4, $Na^+(DXE)_x$, $x = 1$ and 2, and Na^+(12c4).[10,11]

Indeed, the experimental and theoretical values are within experimental error except for the $Na^+(DME)_x$ and $Na^+(DXE)_x$, $x = 1$ and 2, complexes. However, even in the limit that no lifetime shift is observed (the fastest possible dissociation rates), the experimental BDEs for $Na^+(DME)_x$, $x = 1$ and 2, will still not agree with theory. In the case of $Na^+(DXE)$, attaining a BDE that agrees with theory within experimental error limits requires an extremely loose TS, with an entropy of activation of 60 J/(mol K) at 1000 K. This value seems improbable because this $\Delta S^{\dagger}$ value is almost twice that calculated for our *loose* TS, where the TS mode frequencies are divided by 10 and that for the PSL model, which should represent the loosest possible TS. In the case of $Na^+(DXE)_2$, the disagreement between theory and experiment is just outside of experimental error.

A similar comparison between our experimental BDEs and the theoretical values has been made for the analogous Li^+ compounds. In previous work, we have measured and calculated the BDEs of $Li^+(DME)_x$, $x = 1-4$;[12] $Li^+(DXE)_x$, $x = 1$ and 2; and Li^+(12c4).[13] The agreement between the experimental (*loose* TS model) and theoretical values was generally good for the monodentate species (discrepancies ranging from 2 to 12 kJ/mol) and fair for the multidentate species (discrepancies ranging from 13 to 32 kJ/mol). When normalized by the number of oxygen atoms in the ligand, the discrepancies are comparable for mono- and multidentate ligands, 8 ± 5 kJ/mol on average. Del Bene[46] has shown that the accuracy of Li^+ binding affinities is sensitive to the basis set size and to the presence of polarization functions. This was also observed in our previous work,[12,13] where it was found that the discrepancies for the monodentate species decreased when values at the complete basis set (CBS) limit were estimated. The estimated BDE at the CBS limit for the multidentate $Li^+(DXE)$ also yielded a BDE in very good agreement with experiment. BDEs at the CBS limit were not determined or estimated for $Li^+(DXE)_2$ and Li^+(12c4). Although it is not possible to know the effect of changing the basis set size on the calculated BDEs with certainty, in the Li^+ ether complexes, the BDEs calculated at the MP2/6-31+G* level decrease when extrapolated to the CBS limit.[12,13] If this trend continues, theoretical and experimental BDEs will be in even greater accord for the present study as well.

Bonding and Geometry. Several trends can be observed in the experimentally determined BDEs listed in Table 3. Not surprisingly, the bidentate ligand, DXE, is bound more strongly

TABLE 4: Total Bond Dissociation Enthalpies at 298 K of $Na^+(DME)_x$, $x = 2$ and 4; $Na^+(DXE)_x$, $x = 1$ and 2; and $Na^+(12c4)$ in kJ/mol

species	no. of oxygen atoms	ΔH_{298}(PSL)
$Na^+(DME)_2$	2	172 ± 7
$Na^+(DXE)$	2	161 ± 4
$Na^+(DME)_4$	4	297 ± 10
$Na^+(DXE)_2$	4	275 ± 9
$Na^+(12c4)$	4	254 ± 13

to Na^+ than the monodentate DME ligand, and the tetradentate 12c4 ligand exhibits the largest BDE. The BDEs for the $Na^+(DME)_x$ complexes monotonically decrease as x increases. The average drop in the BDEs is 12 ± 3 kJ/mol per additional DME ligand. Likewise, the second DXE ligand is bound 47 ± 9 kJ/mol more loosely than the first, or 24 ± 5 kJ/mol per metal−oxygen interaction. This trend is in agreement with theory and conventional ideas of electrostatic ligation of gas phase ions, viz., BDEs decrease with increasing ligation because of increasing ligand−ligand repulsion and increased charge solvation whereby the effective nuclear charge decreases.[47]

Additional insight into the trends in these BDEs can be obtained by comparing different metal cation ether complexes that contain the same number of carbon and oxygen atoms. $Na^+(DME)_2$ and $Na^+(DXE)$ form one such series, and $Na^+(DME)_4$, $Na^+(DXE)_2$, and $Na^+(12c4)$ comprise another. Table 4 lists these BDEs and BDE sums grouped according to the number of oxygen atoms. In the first case, we compare the sum of BDEs for removing the first and second DME ligands from $Na^+(DME)_2$, 172 ± 7 kJ/mol, with the $Na^+(DXE)$ BDE of 161 ± 4 kJ/mol, Table 4. The difference of 11 ± 8 kJ/mol indicates that the DXE ligand is not bound as well as two DME ligands. A similar observation was made for the analogous Li^+ complexes.[13] We rationalize this result by noting that the DME ligands are free to align their dipoles perfectly to interact with the Na^+ ion core and to adjust the metal−ligand bond distances to optimum lengths. In contrast, the DXE ligand is constrained by the geometry of the ligand such that perfect dipole alignment cannot be achieved. A similar difference of 11 ± 10 kJ/mol is observed between the sum of BDEs for removing the third and fourth DME ligands from $Na^+(DME)_4$, 125 ± 6 kJ/mol, with the $Na^+(DXE)_2$ BDE of 114 ± 8 kJ/mol, Table 3.

In the second series, removing all four DME ligands from $Na^+(DME)_4$ at 298 K requires 22 ± 13 kJ/mol more energy than the sum of the first and second BDEs of $Na^+(DXE)_2$, and 43 ± 16 kJ/mol more than the $Na^+(12c4)$ BDE. Clearly, the most stable structure in this group is $Na^+(DME)_4$. This species has four ligands that can independently align their dipoles and adjust their metal−ligand bond distances with the only constraint coming from steric hindrance with neighboring ligands. The next most stable structure is $Na^+(DXE)_2$, which is more stable than $Na^+(12c4)$ because there are fewer constraints on dipole alignment and M^+−O distance for the DXE species than the 12c4 species.

These results support similar conclusions drawn by Hay et al.,[48,49] who investigated structural requirements for strain-free metal ion complexation with aliphatic ethers using molecular mechanics and *ab initio* methods. They found that the greatest complex stability was achieved when the metal−oxygen length could be optimized and the atoms surrounding the oxygen atoms were oriented in a trigonal planar geometry. Clearly, these preferences can be easily achieved by the independent DME ligands, but are constrained by the preorganized DXE and 12c4 ligands.

Comparison with Literature. Previous experimental studies of the complexes examined in this study have not been performed. Related work concerns the BDEs of $Na^+(H_2O)_x$, $x = 1-4$, which have been determined by Dzidic and Kebarle[4] using high-pressure mass spectrometry and Dalleska et al.[3] using guided ion beam mass spectrometry. The values from these two studies are in good agreement with each other and with theoretical values available from Glendening and Feller.[50] Experimentally and theoretically determined BDEs of $Na^+(DME)_x$, $x = 1-4$, are compared with experimental and theoretical BDEs for $Na^+(H_2O)_x$, $x = 1-4$, in Figure 4. The BDEs for each set of complexes decrease monotonically as x increases. The experimental BDEs for the $Na^+(DME)_x$, $x = 1-4$, are 0.93, 0.93, 1.00, and 1.02 of the respective $Na^+(H_2O)_x$, $x = 1-4$, BDEs. These relative trends differ from results for analogous Li^+ complexes[12] where the $Li^+(DME)_x$, $x = 1-4$, BDEs were 1.18, 1.09, 1.00, and 0.95 of the respective $Li^+(H_2O)_x$, $x = 1-4$, BDEs. The Li^+ result was rationalized by noting that DME has a greater polarizability than H_2O; hence the BDEs for $x = 1$ and 2 are larger for DME than H_2O. As additional ligands are added to Li^+, the larger DME ligands have steric interactions that mediate the polarizability advantage such that the BDEs for $x = 3$ and 4 with DME are comparable to or less than the H_2O BDEs. In the Na complexes, the bond lengths are sufficiently long that the steric interactions apparently do not increase with increasing ligation. Further, the longer bond lengths in the Na complexes mean that the charge-induced dipole interaction (which scales as r^{-4} and dominates the M^+−DME interaction) is relatively less important than the charge−dipole interaction (which scales as r^{-2} and dominates the M^+−H_2O interactions). This apparently causes the $Na^+(DME)_x$ BDEs for $x = 1$ and 2 to be smaller than the $Na^+(H_2O)_x$ BDEs. Further analysis of these trends is currently underway by examining the corresponding BDEs for analogous complexes with K^+, Rb^+, and Cs^+.

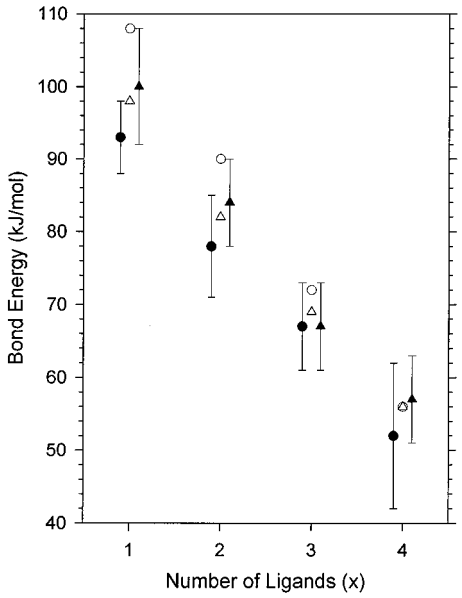

Figure 4. Bond dissociation energies at 0 K (in kJ/mol) of $(R_2O)_{x-1}Na^+-(OR_2)$ where the R_2O ligand is dimethyl ether (R = CH_3, triangles) and water (R = H, circles) plotted vs x. Open and solid symbols refer to experimental and theoretical results, respectively. Bond dissociation energies for $(H_2O)_{x-1}Na^+-(H_2O)$ are taken from ref 3.

The most closely related work in the literature is our studies of $Li^+(DME)_x$, $x = 1-4$,[12] $Li^+(DXE)_x$, $x = 1$ and 2, and $Li^+(12c4)$.[13] The BDEs of the lithium and sodium ion complexes at 298 K (loose transition state values in both cases to allow a direct comparison) are plotted against each other in Figure 5. We find that the BDEs for the singly ligated complexes, $M^+(L)$, are nearly linearly correlated, while those for the multiply

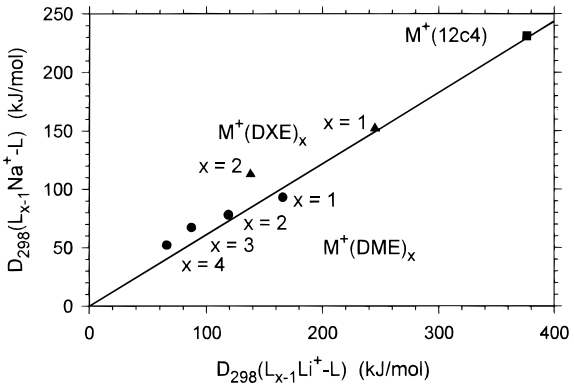

Figure 5. Bond dissociation enthalpies, E_0(loose), at 298 K of sodium vs lithium complexes with dimethyl ether (DME) (circles), 1,2-dimethoxyethane (DXE) (triangles), and 12-crown-4 (12c4) (square). The line is a linear regression analysis of the three monoligated complexes constrained to go through the origin.

ligated complexes, $M^+(L)_x$, fall above this correlation, indicating that the lithium complexes are weaker than expected from this correlation. This can be explained by more dipole−dipole repulsion in the multiligated Li^+ complexes, largely because the ligand−ligand distances are much shorter. This effect is also present in the multidentate complexes, but in these species the dipole repulsion is not as strong because the ligand geometry prevents the dipoles from being optimally oriented toward the metal ion. In the previous work with $Li^+(DXE)_x$, theoretical calculations[13] showed that the Li^+−O bonds are ∼25° from collinear with the C−O−C dipole. Similarly in the Li^+(12c4) species, the Li^+−O bonds are ∼50° from collinear with the C−O−C dipole. In both cases, the C−C backbones of the DXE and 12c4 ligands limit the freedom of the C−O−C dipole orientation.

The BDEs can be decomposed into attractive and repulsive components. The natural energy decomposition analysis (NEDA) of Feller et al.[10−13] helps reveal the subtle differences in the bonding of Li^+ and Na^+ to the DME, DXE, and 12c4 ligands. The attractive components per ligand (i.e., the electrostatic, exchange, and charge transfer terms) for both the $Li^+(DME)_x$ and $Na^+(DME)_x$ species vary little with x showing deviations of only 8 and 11%, respectively. However, the repulsive contributions (i.e., distortion of the ligand geometry, deformation of the metal core, and ligand charge distributions) vary considerably more. For $Li^+(DME)_x$, the repulsive term per ligand increases about 38% from $x = 1$ to 4, but the $Na^+(DME)_x$ species shows only a 9% increase over this range. The same behavior is also noted for the DXE ligands. The differences in the attractive components per ligand for the $M^+(DXE)_2$, $x = 1$ and 2, are 1 and 4%, for M = Li and Na, respectively. The repulsive terms per ligand increase by 34 and 11%, respectively. Evidently, the compact lithium cation distorts the charge distribution and geometry of the DME and DXE ligands much more significantly than the sodium cation. These observations point to why the Li^+ BDEs are weaker than expected when examined relative to the Na^+ BDEs.

Macrocylic Effect. The thermodynamic data obtained here may be useful in providing insight into the macrocyclic effect, which refers to the greater thermodynamic stability of a complex with a cyclic multidentate ligand when compared to the complex formed by a comparable acyclic ligand.[51] It is unknown what contributions are made by the intrinsic metal−ligand binding enthalpies vs the entropic considerations of a preorganized ligand.

In the gas phase, where solvation effects are bypassed, Dearden et al.[7] have shown that reaction rate efficiencies for 1:1 ligand alkali metal cation complexation are greater for cyclic ligands (i.e. crowns) than for the corresponding acyclic glymes. These results are attributed largely to entropic effects, although he adds that further experiments are needed to quantify this conclusion.[9] Our results for Li^+ and Na^+ complexes also suggest that the macrocyclic effect is operative in an entropic sense; that is, rates for formation are faster for complexes aided by the preorganization of the crown ether ring. This conclusion arises from our thermodynamic determination that complexes with greater configurational entropy, such as $M^+(DME)_4$ or $M^+(DXE)_2$ (M = Li or Na), are more stable enthalpically than preorganized structures, such as M^+(12c4). Our results allow us to only speculate about the gas phase macrocyclic effect because our comparisons are between multiple noncyclic mono- and bidentate ligands with a comparable single cyclic tetradentate ligand. To address the gas phase macrocyclic effect most directly, the binding energy of Na^+ to the glymes (analogous acyclic ethers) must be determined.

Conclusion

Kinetic energy dependent collision-induced dissociation in a guided ion beam mass spectrometer is used to determine the absolute bond dissociation energies of sodium cation complexes with one through four dimethyl ether molecules, one and two 1,2-dimethoxyethane molecules, and the 12-crown-4 cyclic polyether. Effects of multiple collisions, internal energies of the complexes, reactant translational energy distributions, and dissociation lifetimes are all accounted for. Kinetic shifts in the measured thresholds increase with the number of ligands in the metal−ligand complex and with increasing bond dissociation energy. Overall, the experimental cross sections and fragmentation pathways observed here are comparable to those previously determined for the analogous complexes with Li^+.[12,13] The only significant difference occurs for the Na^+(12c4) complex, where no ligand dissociation channels are observed, in contrast to the results for Li^+(12c4).

The bond dissociation energies obtained here experimentally are in reasonable agreement with results of *ab initio* calculations,[10,11] with an average deviation of 7 ± 5 kJ/mol per metal−oxygen interaction. Comparison of complexes containing the same number of metal−oxygen interactions shows that the preorganized multidentate ligands bind less tightly than the monodentate ligands, an effect attributed to geometric constraints in the former systems. Comparison of the trends in the bond dissociation energies between the Li^+ and Na^+ complexes shows the expected result that complexes with the smaller lithium ion have significantly greater BDEs than the comparable sodium ion complexes. Further, there is evidence for more ligand−ligand repulsion in the multiply ligated Li^+ complexes.

Acknowledgment. Funding for this work was provided by the National Science Foundation under Grant No. CHE-9530412 (P.B.A.) and by the Division of Chemical Sciences, Office of Basic Energy Sciences, U.S. Department of Energy (M.B.M., D.R.). Pacific Northwest National Laboratory is operated for the U.S. Department of Energy by Battelle under Contract DE-AC06-76RLO 1830.

References and Notes

(1) See: *Principles of Molecular Recognition*; Buckingham, A. D., Roberts, S. M., Eds.; Blackie Academic and Professional: Glasglow, 1993.

(2) Izatt, R. M.; Rytting, J. H.; Nelson, D. P.; Haymore, B. L.; Christensen, J. J. *Science* **1969**, *164*, 443. Izatt, R. M.; Bradshaw, J. S.; Nielsen, S. A.; Lamb, J. D.; Christensen, J. J.; Sen, D. *Chem. Rev.* **1985**, *85*, 271. Izatt, R. M.; Pawlak, K.; Bradshaw, J. S.; Bruening, R. L. *Chem Rev.* **1991**, *91*, 1721.

(3) Dalleska, N. F.; Tjelta, B. L.; Armentrout, P. B. *J. Phys. Chem.* **1994**, *98*, 4191.
(4) Dzidic, I.; Kebarle, P. *J. Chem. Phys.* **1970**, *74*, 1466.
(5) Maleknia, S.; Brodbelt, J. *J. Am. Chem. Soc.* **1992**, *114*, 4295. Liou, C.-C.; Brodbelt, J. S. *Pure Appl. Chem.* **1993**, *65*, 409.
(6) Cooks, R. G.; Kruger, T. L. *J. Am. Chem. Soc.* **1977**, *99*, 1279.
(7) Dearden, D. V.; Zhang, H.; Chu, I.-C.; Chen, Q. *Pure Appl. Chem.* **1993**, *65*, 423.
(8) Chu, I.-H; Zhang, H.; Dearden, D. V. *J. Am. Chem. Soc.* **1993**, *115*, 5736.
(9) Zhang, H.; Dearden, D. V. *J. Am. Chem. Soc.* **1992**, *114*, 2754.
(10) Hill, S. E.; Glendening, E. D.; Feller, D. Submitted to *J. Phys. Chem.*
(11) Glendening, E. D.; Hill, S. E.; Feller, D. Submitted to *J. Phys. Chem.*
(12) More, M. B.; Glendening, E. D.; Ray, D.; Feller, D.; Armentrout, P. B. *J. Phys. Chem.***1996**, *100*, 1605.
(13) Ray, D.; Feller, D.; More, M. B.; Glendening, E. D.; Armentrout, P. B. *J. Phys. Chem.* **1996**, *100*, 16116.
(14) Ervin, K. M.; Armentrout, P. B. *J. Chem. Phys.* **1985**, *83*, 166.
(15) Shultz, R. H.; Armentrout, P. B. *Int. J. Mass Spectrom. Ion Processes* **1991**, *107*, 29.
(16) Aristov, N.; Armentrout, P. B. *J. Phys. Chem.* **1986**, *90*, 5135.
(17) Dalleska, N. F.; Honma, K.; Sunderlin, L. S.; Armentrout, P. B. *J. Am. Chem. Soc.* **1994**, *116*, 3519.
(18) Chantry, P. J. *J. Chem. Phys.* **1971**, *55*, 2746.
(19) Shultz, R. H.; Armentrout, P. B. *J. Chem. Phys.* **1992**, *96*, 1046.
(20) Shultz, R. H.; Crellin, K. C.; Armentrout, P. B. *J. Am. Chem. Soc.* **1991**, *113*, 8590.
(21) Khan, F. A.; Clemmer, D. C.; Schultz, R. H.; Armentrout, P. B. *J. Phys. Chem.* **1993**, *97*, 7978.
(22) Fisher, E. R.; Kickel, B. L.; Armentrout, P. B. *J. Phys. Chem.* **1993**, *97*, 10204.
(23) Fisher, E. R.; Kickel, B. L.; Armentrout, P. B. *J. Chem. Phys.* **1992**, *96*, 4859.
(24) Beyer, T. S.; Swinehart, D. F. *Comm. Assoc. Comput. Machines* **1973**, *16*, 379. Stein, S. E.; Rabinovitch, B. S. *J. Chem. Phys.* **1973**, *58*, 2438. Stein, S. E.; Rabinovitch, B. S. *Chem. Phys. Lett.* **1977**, *49*, 183. Gilbert, R. G.; Smith, S. C. *Theory of Unimolecular and Recombination Reactions*; Blackwell Scientific Publications: Oxford, 1990.
(25) Shimanouchi, T. *Tables of Molecular Vibrational Frequencies: Consolidated Volume I*; NSRDS-NBS 39; U.S. Government Printing Office: Washington, DC, 1972.
(26) Chesvnavich, W. J.; Bowers, M. T. *J. Phys. Chem.* **1979**, *83*, 900.
(27) Armentrout, P. B. In *Advances in Gas Phase Ion Chemistry*; Adams, N. G., Babcock, L. M., Eds.; JAI: Greenwich, 1992; Vol. 1, pp 83−119.
(28) See for example: Sunderlin, L. S.; Armentrout, P. B. *Int. J. Mass Spectrom. Ion Processes* **1989**, *94*, 149.
(29) Weber, M. E.; Elkind, J. L.; Armentrout, P. B. *J. Chem. Phys.* **1986**, *84*, 1521.
(30) Hales, D. A.; Lian, L.; Armentrout, P. B. *Int. J. Mass Spectrom. Ion Processes* **1990**, *102*, 269.
(31) Rodgers, M. T.; Ervin, K. M.; Armentrout, P. B. *J. Chem. Phys.*, accepted for publication.
(32) Rodgers, M. T.; Armentrout, P. B. *J. Phys Chem.*, accepted for publication.
(33) Rodgers, M. T.; Armentrout, P. B. *J. Phys. Chem.*, submitted for publication.
(34) Dalleska, N. F.; Honma, K.; Armentrout, P. B. *J. Am. Chem. Soc.* **1993**, *115*, 12125. See Figure 1 of this reference.
(35) Boo, B. H.; Armentrout, P. B. *J. Am. Chem. Soc.* **1987**, *109*, 3459. Ervin, K. M.; Armentrout, P. B. *J. Chem. Phys.* **1987**, *86*, 2659. Elkind, J. L.; Armentrout, P. B. *J. Phys. Chem.* **1984**, *88*, 5454. Armentrout, P. B. In *Structure/Reactivity and Thermochemistry of Ions*; Ausloos, P., Lias, S. G., Eds.; Reidel: Dordrecht, 1987; pp 97−164.
(36) Armentrout, P. B.; Simons, J. *J. Am. Chem. Soc.* **1992**, *114*, 8627.
(37) Chase, M. W.; Davies, C. A.; Downey, J. R.; Frurip, D. J.; McDonald, R. A.; Syverud, A. N. *J. Phys. Chem. Ref. Data* **1985**, *14*, Suppl. 1.
(38) Meyer, F.; Khan, F. A.; Armentrout, P. B. *J. Am. Chem. Soc.* **1995**, *117*, 9740.
(39) Malinovich, Y.; Liftshitz, C. *J. Phys. Chem.* **1986**, *90*, 2200.
(40) Ziesel, J. P.; Liftshitz, C. *J. Chem. Phys.* **1987**, *117*, 227.
(41) Hase, W. L.; Richou, M.; Mondro, S. L. *J. Phys. Chem.* **1989**, *93*, 539.
(42) Lian, L.; Su, C.-X.; Armentrout, P. B. *J. Chem. Phys.* **1992**, *6*, 4072.
(43) Lian, L.; Su, C.-X.; Armentrout, P. B. *J. Chem. Phys.* **1992**, *6*, 4084.
(44) Robinson, P. J.; Holbrook, K. A. *Unimolecular Reactions*; Wiley-Interscience: New York, 1972.
(45) Hehre, W. J.; Ditchfield, R.; Pople, J. A. *J. Chem. Phys.* **1972**, *56*, 2257.
(46) Del Bene, J. E. *J. Phys. Chem.* **1996**, *100*, 6284.
(47) See natural energy decomposition analysis of $Li^+(DME)_x$ clusters in ref 12.
(48) Hay, B. P.; Rustad, J. R. *J. Am. Chem. Soc.* **1994**, *116*, 6316.
(49) Hay, B. P.; Rustad, J. R.; Hostetler, C. J. *J. Am. Chem. Soc.* **1993**, *115*, 11158.
(50) Glending, E. D.; Feller, D. *J. Phys. Chem.* **1995**, *99*, 3060.
(51) Cotton, F. A.; Wilkinson, G. *Advanced Inorganic Chemistry*, 5th ed.; John Wiley and Sons: New York, 1988; p 47.